

# Orthogonally polarized optical single sideband modulation for microwave photonics processing using stimulated Brillouin scattering

Mikel Sagues and Alayn Loayssa\*

Departamento de Ingeniería Eléctrica y Electrónica,  
Universidad Pública de Navarra Campus Arrosadia s/n,  
31006 Pamplona Spain  
\*alayn.loayssa@unavarra.es  
[www.unavarra.es](http://www.unavarra.es)

**Abstract:** We present a novel technique to generate orthogonally polarized optical single sideband modulated signals. The modulation scheme is based on all optical stimulated Brillouin scattering processing of the optical carrier of an optical single sideband modulated signal, by means of the polarization state dragging induced by this non-linear effect. This modulation technique can be used in several microwave photonics applications, such as antenna beamforming or microwave photonics filters. In order to perform a proof-of-concept experiment, the orthogonal modulator is deployed for the implementation of an RF phase-shifter.

© 2010 Optical Society of America

**OCIS codes:** (999.9999) Single sideband modulation; (290.5900) Scattering, stimulated Brillouin; (070.1170) Analog optical signal processing; (070.4340) Nonlinear optical signal processing; (060.4370) Nonlinear optics, fibers; (999.9999) Microwave photonics.

---

## References and links

1. G. H. Smith, D. Novak, and Z. Ahmed, "Technique for optical SSB generation to overcome dispersion penalties in fibre-radio systems," *Electron. Lett.* **33**(1), 74–75 (1997).
2. A. Loayssa and F. J. Lahoz, "Broad-band RF photonic phase shifter based on stimulated Brillouin scattering and single-sideband modulation," *IEEE Photon. Technol. Lett.* **18**(1), 208–210 (2006).
3. J. Mora, J. Capmany, A. Loayssa, and D. Pastor, "Novel technique for implementing incoherent microwave photonic filters with negative coefficients using phase modulation and single sideband selection," *IEEE Photon. Technol. Lett.* **18**(18), 1943–1945 (2006).
4. A. Loayssa, J. Capmany, M. Sagues, and J. Mora, "Demonstration of incoherent microwave photonic filters with all-optical complex coefficients," *IEEE Photon. Technol. Lett.* **18**(16), 1744–1746 (2006).
5. M. Sagues, R. García Olcina, A. Loayssa, S. Sales, and J. Capmany, "Multi-tap complex-coefficient incoherent microwave photonic filters based on optical single-sideband modulation and narrow band optical filtering," *Opt. Express* **16**(1), 295–303 (2008), <http://www.opticsinfobase.org/oe/abstract.cfm?URI=oe-16-1-295>.
6. M. Sagues, M. Pérez, and A. Loayssa, "Measurement of polarization dependent loss, polarization mode dispersion and group delay of optical components using swept optical single sideband modulated signals," *Opt. Express* **16**(20), 16181–16188 (2008), <http://www.opticsinfobase.org/oe/abstract.cfm?URI=oe-16-20-16181>.
7. D. Dolfi, P. Joffre, J. Antoine, J. P. Huignard, D. Philippon, and P. Granger, "Experimental demonstration of a phased-array antenna optically controlled with phase and time delays," *Appl. Opt.* **35**(26), 5293–5300 (1996).
8. B. Vidal, T. Mengual, C. Ibanez-Lopez, and J. Martí, "Optical Beamforming Network Based on Fiber-Optical Delay Lines and Spatial Light Modulators for Large Antenna Arrays," *IEEE Photon. Technol. Lett.* **18**(24), 2590–2592 (2006).
9. T. Mengual, B. Vidal, and J. Martí, "Continuously tunable photonic microwave filter based on a spatial light modulator," *Opt. Commun.* **281**, 2746–2749 (2008).
10. Z. Li, C. Yu, Y. Dong, L. Cheng, L. F. K. Lui, C. Lu, A. P. Lau, H. Y. Tam, and P. K. Wai, "Linear photonic radio frequency phase shifter using a differential-group-delay element and an optical phase modulator," *Opt. Lett.* **35**(11), 1881–1883 (2010).
11. A. L. Campillo, "Orthogonally polarized single sideband modulator," *Opt. Lett.* **32**(21), 3152–3154 (2007).
12. L. Thévenaz, A. Zadok, A. Eyal, and M. Tur, "All-optical polarization control through Brillouin amplification," in Proc. *Optical Fiber Communications Conference*, (OFC'2008) paper OML7 (2008).
13. A. Zadok, E. Zilka, A. Eyal, L. Thévenaz, and M. Tur, "Vector analysis of stimulated Brillouin scattering amplification in standard single-mode fibers," *Opt. Express* **16**(26), 21692–21707 (2008), <http://www.opticsinfobase.org/oe/abstract.cfm?URI=oe-16-26-21692>.

14. T. Kawanishi, T. Sakamoto, A. Chiba, M. Izutsu, K. Higuma, J. Ichikawa, T. Lee, and V. Filsinger, "High-speed dual-parallel Mach-Zehnder Modulator using Thin Lithium Niobate Substrate," in Proc. *Optical Fiber Communications Conference*, (OFC'2008) paper JThA34 (2008).
15. M. O. Deventer and A. J. Boot, "Polarization properties of stimulated Brillouin scattering in single-mode fibers," *J. Lightwave Technol.* **12**(4), 585–590 (1994).

## Introduction

Modulation formats other than the standard double sideband intensity modulation have been proposed in order to improve the performance of optical systems and for optical signal processing applications. Among them, optical single sideband (OSSB) modulation has been a field of increasing interest in the last years [1–11].

Recently, the use of orthogonally polarized OSSB modulated signals for microwave processing schemes has been proposed, with applications in antenna beamforming and in microwave photonics filters implementing complex coefficients [7–10]. Ideally, in this modulation scheme, the state of polarization (SOP) of the modulation sideband is orthogonal to that of the optical carrier. Existing proposals for microwave photonics processing using orthogonal OSSB modulation are mainly based on spatial light modulation technologies. These offer the promise of parallel signal processing and a compact integration. The first proposal used an acoustic modulator for the generation of orthogonally polarized optical carrier and single-sideband signal [7]. A recent upgrade of this proposal is based on using a differential group delay (DGD) module to get orthogonal polarizations in an OSSB modulated signal [8–10]. The main drawback of these systems is that their bandwidth is limited either by the acoustic modulator or by the DGD module, which only provide orthogonal polarization in a certain RF frequency range. Other orthogonal OSSB modulation schemes are based on special polarization modulators [11].

In this work, we introduce a technique that provides broadband orthogonal modulation by applying stimulated Brillouin scattering (SBS) processing to any given conventional OSSB modulation scheme. The orthogonal modulation scheme is based on a recently proposed technique to control the state of polarization (SOP) of optical signals through Brillouin amplification [12,13]. In this paper, the orthogonal modulation technique is applied to the implementation of an all optical RF phase-shifter.

## Fundamentals

The fundamentals of the orthogonal modulation technique are schematically depicted in Fig. 1. A conventional OSSB modulated signal, generated by any of the techniques proposed in the literature, goes through the orthogonal modulator. This is composed of a spool of  $L$  km of low birefringent fiber, a circulator and a pump wave whose SOP is tuned with a polarization controller (PC). The optical frequency of the pump wave is detuned from the optical carrier of the OSSB modulation by the fiber's Brillouin frequency shift. Both signals are counterpropagated in the spool of fiber using a circulator, so that the optical carrier is amplified due to Brillouin interaction.

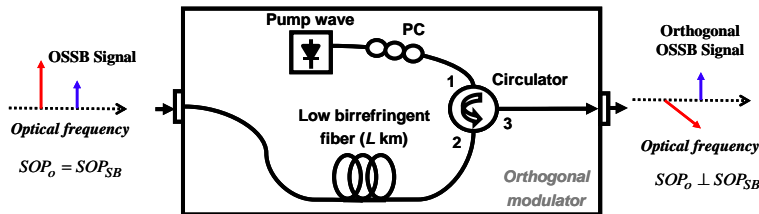


Fig. 1. Fundamentals of the narrowband optical processing of the optical carrier for the implementation of an OSSB orthogonal modulator.  $SOP_o$ : SOP of optical carrier;  $SOP_{SB}$ : SOP of modulation sideband.

When SBS amplification is applied to an optical signal, the amplified signal tends to drag its SOP towards the SOP of the pump signal [12]. The degree of matching with the pump SOP

varies as a function of SBS signal amplification and the relationship between the unprocessed SOP of the signal and the pump. However, for high Brillouin amplifications ( $> 30$  dB), the SOP of the signal can be kept very near to that of the pump signal [12]. In the proposed technique, the modulation sideband is not altered as long as the modulation frequency is higher than the Brillouin linewidth, which is of the order of a few tens of megahertz at 1550 nm. Therefore, if the SOP of the pump in Fig. 1 is set orthogonal to the SOP of the unprocessed signal, the SOP of the optical carrier is dragged towards the SOP of the pump, while the SOP of the sideband remains unaltered. In that way, a broadband orthogonal OSSB modulation is achieved, whose bandwidth of operation is only limited by that of the original OSSB modulation.

An orthogonal OSSB modulation as described above can be deployed to introduce a broadband phase-shift into an RF signal, by means of the correspondence or mapping between the optical and the electrical domain provided by OSSB modulation [2]. Broadband phase shifters are needed, for instance, in phased-array beamforming and in signal processing for broadband electronic applications. In order to control the phase-shift of several RF signals (antenna elements, or filter taps) with a single optical device, parallel alignment spatial light modulators (PAL-SLM) can be deployed in combination with orthogonal OSSB modulation [8,9]. Figure 2 depicts the principle behind the technique. If one polarization component of the orthogonally modulated light impinging on the PAL-SLM is aligned with the axis of the liquid-crystal molecules, the PAL-SLM can change the refraction index experienced by this signal according to the applied voltage. On the other side, light polarized along the orthogonal polarization undergoes a constant refraction index. If both signals are combined in an optical polarizer and detected in a photodetector, the optical phase-shift applied to the signal on the tunable-refraction-index axis, is translated to the recovered RF signal [8]. Therefore, by changing the voltage applied to the PAL-SLM, the phase-shift of the RF signal can be continuously tuned.

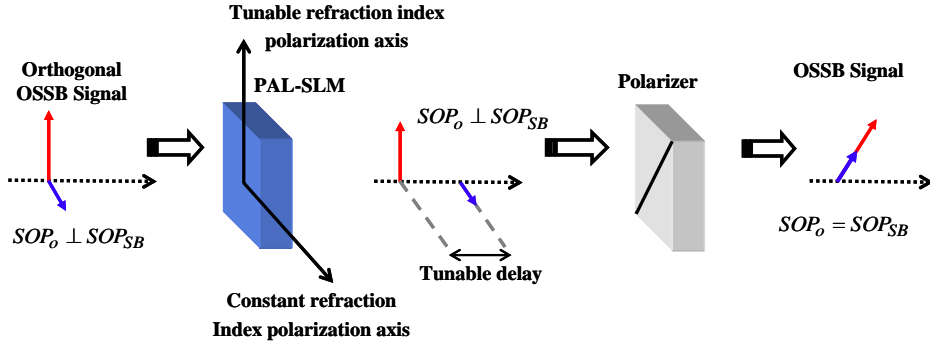


Fig. 2. Schematic description of the RF phase-shifting technique. The refraction index seen by the optical signal in one of the axis can be tuned, while the other remains unaltered.

The previous technique requires that the SOP of the optical carrier and the sideband are perfectly orthogonal. However, to obtain such a perfect orthogonal modulation by SBS polarization dragging would require of extremely high pump powers, due to the fact that this dragging is relatively small when the pump wave and the original optical carrier at the output of the fiber are perfectly orthogonal [13]. In order to evaluate the effect of the latter, we study the case where the processing described in Fig. 2 is performed with a non-perfectly orthogonal OSSB signal. This case is schematically depicted in Fig. 3. For the sake of simplicity, both SOP of optical carrier and sideband are considered to be linear in relation to the polarization axes of the PAL-SLM which are chosen as the reference axes for the theoretical derivations. Besides, only the optical carrier and the main modulation sideband of the OSSB signal will be considered. The optical carrier's SOP is aligned with the constant refraction index axis of the PAL-SLM. The angle  $\rangle$  measures the orthogonality between the sideband and the optical carrier of the modulation, and the angle  $\rightarrow$  represents the alignment of the polarizer in relation

to the constant refraction index axis of the PAL-SLM. Finally,  $\phi$  represents the differential optical phase-shift seen by optical carrier and sideband, which will be a function of the differential delay in the two orthogonal axes.

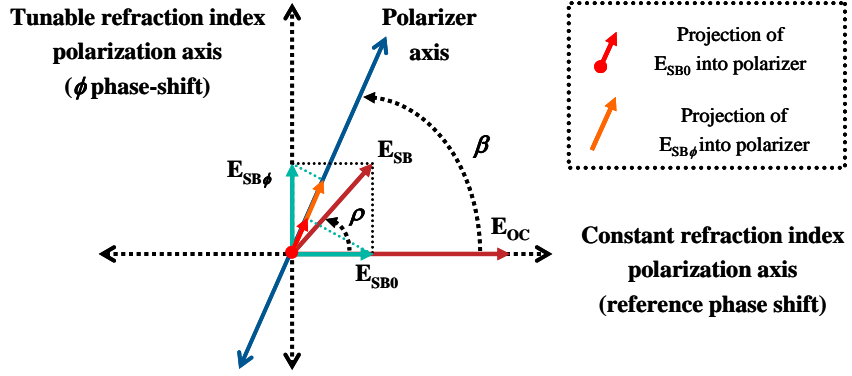


Fig. 3. Graphical representation of the fundamentals of the optical processing for the RF phase-shifter showing the addition of both desired and interfering terms in Eq. (3).  $E_{oc}$ : electric field of the optical carrier;  $E_{sb}$ : electric field of the sideband;  $E_{sb\phi}$ : projection of the electric field of the sideband into the tunable refraction index axis;  $E_{sb0}$ : projection of the electric field of the sideband into the constant refraction index axis.

Mathematically, this processing can be expressed with the following equations for the electric fields of the sideband  $\vec{E}_{sb}(t)$  and of the optical carrier  $\vec{E}_{oc}(t)$  at the output of the system:

$$\begin{aligned}\vec{E}_{oc}(t) &= A_{oc} \cdot \begin{pmatrix} \cos^2(\beta) & \cos(\beta) \cdot \sin(\beta) \\ \cos(\beta) \cdot \sin(\beta) & \cos^2(\beta) \end{pmatrix} \cdot \begin{pmatrix} 1 & 0 \\ 0 & e^{j\varphi} \end{pmatrix} \cdot \begin{pmatrix} 1 \\ 0 \end{pmatrix} \cdot e^{j \cdot 2\pi \cdot v_o \cdot t} \\ \vec{E}_{sb}(t) &= A_{sb} \cdot \begin{pmatrix} \cos^2(\beta) & \cos(\beta) \cdot \sin(\beta) \\ \cos(\beta) \cdot \sin(\beta) & \cos^2(\beta) \end{pmatrix} \cdot \begin{pmatrix} 1 & 0 \\ 0 & e^{j\varphi} \end{pmatrix} \cdot \begin{pmatrix} \cos(\rho) & -\sin(\rho) \\ \sin(\rho) & \cos(\rho) \end{pmatrix} \cdot \begin{pmatrix} 1 \\ 0 \end{pmatrix} \cdot e^{j \cdot 2\pi \cdot (v_o + f_{RF}) \cdot t}\end{aligned}\quad (1)$$

where  $A_{oc}$  and  $A_{sb}$  are the optical field amplitudes for the optical carrier and sideband,  $v_o$  is the optical frequency of the carrier and  $f_{RF}$  the modulation frequency of the OSSB signal. When this optical signal is photodetected, the received electric current will be proportional to:

$$i(t) \propto \Re \cdot \langle \vec{E}(t)^2 \rangle = \Re \cdot \vec{E}(t)^{*T} \cdot \vec{E}(t) \quad (2)$$

where  $\vec{E}(t) = \vec{E}_{oc}(t) + \vec{E}_{sb}(t)$ ,  $\Re$  is the responsivity of the photodetector and  $\vec{E}(t)^{*T}$  represents the complex-conjugate transpose of  $\vec{E}(t)$ .

As shown in Fig. 3, when  $\beta$  is different from  $90^\circ$ , a different optical phase-shift is applied to each of the projections of the sideband in the polarization axes of the PAL-SLM. These two electric fields will be combined in the polarizer. Therefore, the resulting RF signal's phase-shift will be a function of  $\phi$  and of the amplitude of both projections. Substituting Eq. (1) in Eq. (2), and using fasorial notation, this electric current is found to be proportional to:

$$I(f_{RF}) \propto A_{oc} \cdot A_{sb} \cdot \cos(\beta) \cdot (\cos(\rho) \cdot \cos(\beta) + \sin(\rho) \cdot \sin(\beta) \cdot e^{j\varphi}) \quad (3)$$

For the purpose of the processing we want to apply to the RF signal, the expression between brackets in Eq. (3) can be considered as a term where the desired phase-shift is

applied, proportional to  $\sin(\rho) \cdot \sin(\beta)$ , plus an interference term  $\cos(\rho) \cdot \cos(\beta)$ . Therefore, the recovered RF phase-shift ( $\phi_m$ ) will differ from the applied differential optical phase-shift between optical carrier and sideband ( $\phi$ ). However, if the processing optical phase-shift can be continuously tuned in a  $360^\circ$  range (as is the case where a PAL-SLM is deployed), any given RF phase-shift can be achieved in the recovered RF signal. Therefore, the deviation between applied optical phase-shift and the recovered RF phase-shift imposes no limitation to the RF phase-shifting capability of the system.

A second consequence of the interfering term in Eq. (3) is that the detected RF power will change as a function of the optical phase-shift introduced in the tunable refraction index axis of the PAL-SLM. When multiple OSSB signals are to be controlled with a single PAL-SLM, their amplitude cannot be tuned independently. Therefore, for the multi-beam case, the amplitude error of the system can be defined as the excursion in RF power for all possible  $\phi$ .

Figure 4 shows the RF phase-shift deviation from the applied optical phase-shift and the variation of the detected RF power as a function of  $\phi$  for the case where  $\rho = 45^\circ$  and  $\beta = 89^\circ$ . As expected from Eq. (3), the maximum phase-shift deviation occurs when  $\phi = 90^\circ$  or  $\phi = 270^\circ$ , and the maximum RF power excursion is between  $\phi = 180^\circ$  and  $\phi = 0^\circ$ . Notice that even if the orthogonality of the sideband and the optical carrier is not very high, the recovered RF phase-shift can be arbitrarily tuned. Furthermore, the amplitude error in the system can be kept within reasonable limits by setting the axis of the polarizer near the tunable refraction index axis of the PAL-SLM. However, this will produce a significant attenuation on the optical carrier, and therefore on the detected RF signal. Figure 5 shows the optical carrier attenuation as a function of  $\rho$  and for different amplitude error goals in the system. The optical attenuation is bigger as  $\rho$  decreases and as the amplitude error goal is reduced. For example, for the case where we want to limit the amplitude error to less than 0.1 dB, and having the sideband SOP to  $45^\circ$  of the optical carrier, an attenuation above 20 dB must be applied to the optical carrier. However, this attenuation is not a big issue for the SBS orthogonal modulator, provided that an even higher amplification of the optical carrier must be introduced in order to change its SOP [13].

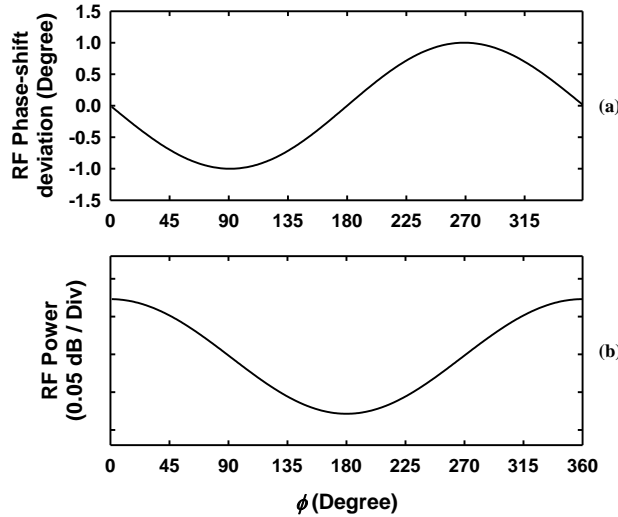


Fig. 4. (a) RF phase-shift deviation from the applied optical phase-shift and (b) detected RF power as a function of  $\phi$  when  $\rho = 45^\circ$  and  $\beta = 89^\circ$ .

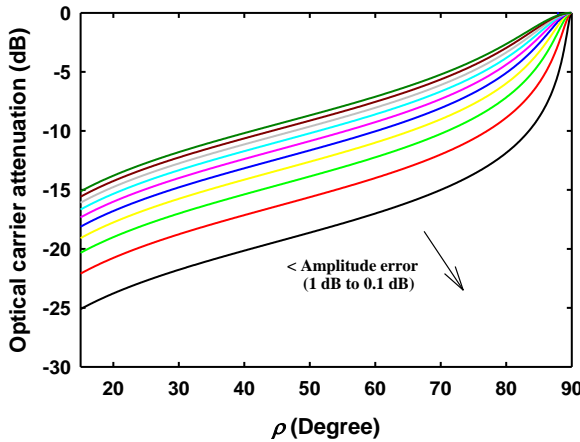


Fig. 5. Optical carrier attenuation as a function of  $\rho$  and for different amplitude error goals in the system, from 1 dB (higher trace) to 0.1 dB.

### Experimental setup and measurements

Due to the narrow bandwidth of SBS interaction, the frequency tuning of the pump and Stokes waves must be controlled with high accuracy. The setup used to experimentally demonstrate a photonic phase-shifter using the orthogonal modulator is outlined in Fig. 6, where all the optical waves are generated from a single laser source [2]. In this way, any wavelength drift of the optical carrier is equally translated to the two counterpropagating signals, so that the stability of the system is granted. The output of a laser source is divided in two paths by a fiber optic coupler. The lower path goes to an OSSB modulator driven by the RF signal to be phase-shifted. The signal in the upper path goes to a dual parallel Mach Zehnder electrooptic modulator (MZ-EOM), which is driven by a microwave generator of frequency  $f_e$  and biased in order to generate an optical single-sideband suppressed carrier (OSSB-SC) signal [14]. A circulator is used to counterpropagate this OSSB-SC signal with the OSSB signal in a 24 Km length of standard singlemode fiber (S-SMF).  $f_e$  is tuned to the Brillouin frequency-shift of the fiber at the wavelength of operation, so that SBS interaction takes place between the sideband of the OSSB-SC, which acts as pump wave, and the optical carrier of the lower branch. Therefore, the wavelength of the optical signals involved in the processing is precisely controlled by the RF modulation frequencies of the two modulators. A polarization controller is used to set the SOP of the pump wave in order to control the SOP of the processed optical carrier at the output of the fiber. An EDFA is used in the upper branch, so that the required pump power is achieved.

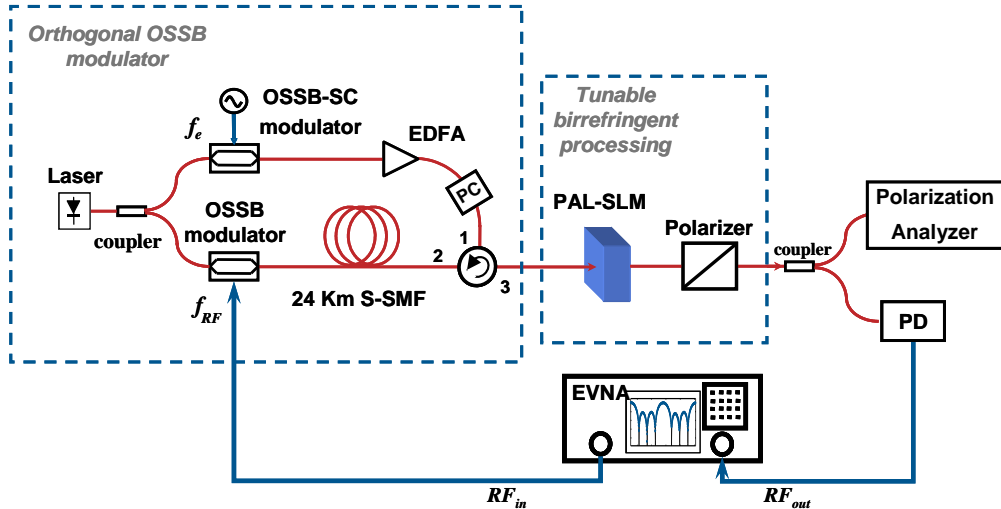


Fig. 6. Experimental setup.

Figure 7 shows the 10-pm resolution spectra of the two counterpropagating signals (OSSB and OSSB-SC) at their respective input ports of the fiber. For the OSSB modulated signal, more than 20 dB of sideband suppression was achieved in the whole modulation range (from 2 GHz to 8 GHz) which was limited by the bandwidth of the deployed MZ-EOM. For the OSSB-SC modulated signal, the optical carrier and the unwanted sideband remain more than 45 dB below the processing sideband, so that any interference due to them is avoided.

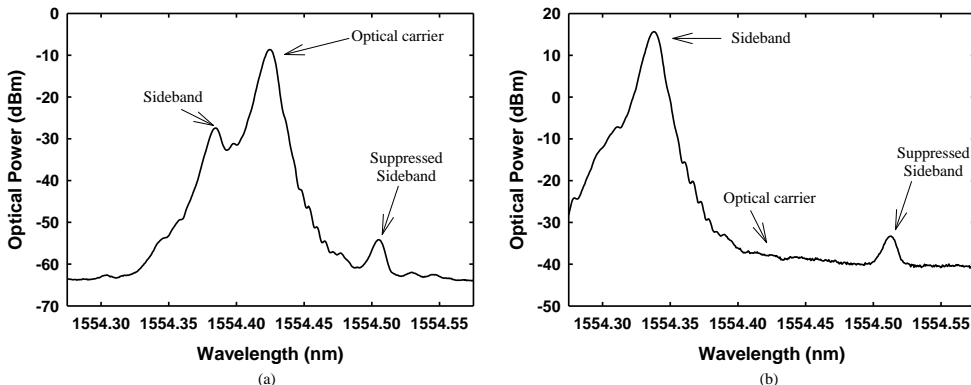


Fig. 7. Measured spectra of the (a) OSSB for a 5 GHz RF modulation frequency and (b) OSSB-SC signals at their respective input ports of the fiber. The center of each graph corresponds to the optical carrier wavelength.

Unfortunately, no PAL-SLM was available in the laboratory. Instead of that, a bulk optics fiber bench from OFR was used to perform the orthogonal phase-shift processing required by the technique. Different retarder waveplates can be introduced in the fiber bench, so that a tunable optical phase-shift is introduced between the two orthogonal SOP of the OSSB modulated signal. In order to combine the sideband and the optical carrier, a polarizer is introduced in the fiber bench. This also allows for an easy tuning of the polarization axis of the polarizer.

A polarization analyzer is used to measure the SOP of the signals involved in the processing. Figure 8 shows the SOP in the Poincaré sphere of the modulation sideband and optical carrier (marked as A) when no SBS processing is applied to the OSSB signal of the

lower branch of the setup and when neither the waveplates nor the polarizer are introduced in the fiber bench. Point B depicts the SOP of the optical carrier when the upper branch signal in the setup is switched on, so that its SOP is dragged towards the SOP of the pump signal, while the sideband SOP remains in point A. Point E marks the SOP of the complex-conjugate of the processing OSSB-SC signal [13]. This was measured by switching off the signal on the lower branch so that spontaneous SBS was excited, acting as a polarization mirror of the pump signal [15]. Notice that the SOP of the optical carrier has been detuned only  $45^\circ$  from its original SOP, even if a better orthogonalization of both components can be easily performed by raising the pump power and tuning the SOP of the complex-conjugate of the pump signal close to the orthogonal SOP of the unprocessed OSSB signal [13]. Points C and D mark the SOP of the OSSB signal after passing through the polarizer, for two different polarization axis alignments. Both of them are tuned near the orthogonal SOP of the optical carrier so that the RF phase-shift and amplitude error is minimized according to Eq. (3).

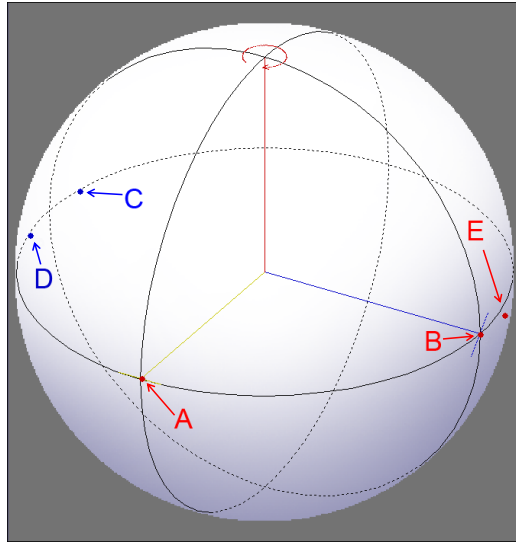


Fig. 8. Poincaré sphere showing the measured SOP of (A) sideband and unprocessed optical carrier, (B) optical carrier when SBS processing is applied, (E) complex-conjugate of OSSB-SC signal and (C, D) polarizer axis.

Finally, the phase-shifted RF signal is recovered in an electric vector network analyzer (EVNA), after detecting the output signal in a 7-GHz photoreceiver. Measurements of the RF phase-shift as two different wave plates ( $\perp/4$  and  $\perp/2$ ) are introduced in the setup are displayed in Fig. 9(a), introducing an RF phase-shift of  $90^\circ$  and  $180^\circ$  respectively, for the case where the polarizer is set so that the SOP of the resulting signal is in D in Fig. 8. From Eq. (3) it can be seen that when  $\beta$  is close to  $90^\circ$  (so that the interfering term is negligible), and as a function of the sign of  $\cos(\beta)$ ,  $180^\circ$  are added to the applied optical phase-shift  $\phi$ . Therefore, if the polarizer is tuned to C in Fig. 8,  $180^\circ$  must be added to the previous phase-shifts resulting in a  $270^\circ$  and  $360^\circ$  phase-shift in the recovered RF signal. Figure 9(b) shows the detected RF power at the EVNA for the four cases described above. A relatively small power variation is observed. Notice that, as predicted by theory, the phase-shift and RF power are nearly independent of RF frequency within the bandwidth of the OSSB modulator. However, a bigger power variation and a lower accuracy in the recovered RF phase-shift are observed when the  $\perp/4$  wave plate is deployed. This is attributed to the bad alignment of the available  $\perp/4$  wave plate with the axis of the fiber bench. This didn't allow for a correct alignment of the SOP of the optical carrier with the axes of the wave plate, introducing an error in the measurement.

In the experiment we were limited by the available orthogonal processing device but, in principle, using PAL-SLM the phase-shift can be continuously tuned in a full phase-shift range ( $360^\circ$ ). Moreover, the use of this device would provide the capability to control several RF signals with a single device.

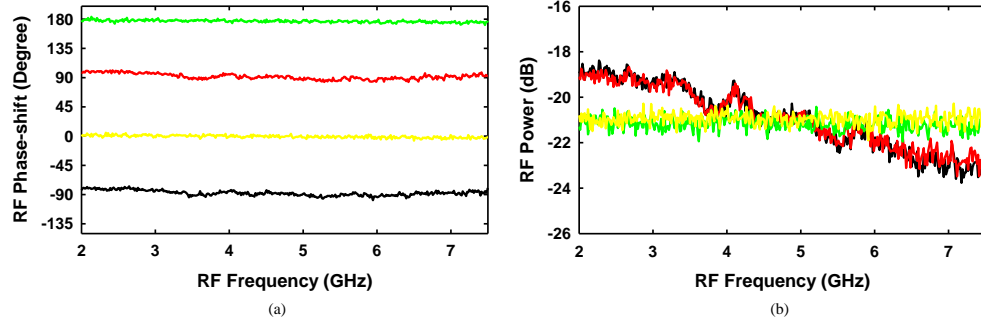


Fig. 9. (a) RF phase-shift tuning and (b) RF power as the retarder wave plate is changed in the setup ( $\lambda/4$  and  $\lambda/2$ ) and as the SOP of the polarizer is tuned from C to D in Fig. 8.

## Conclusions

We have proposed a technique to generate broadband OSSB orthogonal modulation from a conventional OSSB modulated signal, by controlling the SOP of the optical carrier using SBS effect. To the authors' knowledge, this is the first application of SBS control of the SOP of optical signals [12]. The limitations of the modulation technique in relation to the non-orthogonality of the optical carrier and sideband have been studied, showing that very good results can be obtained even if the modulation is not perfectly orthogonal.

A simple proof-of-concept experiment has been performed to demonstrate the capabilities of this technique, implementing an RF phase-shifter.

The SBS modulation orthogonalization technique has been applied to an OSSB signal, but the same concept can also be adapted to achieve any other modulation format. Moreover, multi-beam operation could also be possible, once the effect of wavelength dependence of SBS in the technique is carefully studied.

Further research should focus on the study of other narrowband optical processing techniques which could provide a similar SOP dragging of the optical carrier.

## Acknowledgements

The authors wish to acknowledge the financial support from the Spanish Ministerio de Educación y Ciencia through the projects TEC2007-67987-C02-02 and TEC2010-20224-C02-01.